高温顕微鏡を利用したその場の観察によるCaO滓化メカニズムの解明

Clarification of the Mechanism of CaO-containing Slag Formation *in situ* Observed by High Temperature Optical Microscope

研究代表者　名古屋大学大学院工学研究科　助教授　楊　健

共同研究者　名古屋大学大学院工学研究科　教授　　桑原　守

1. Introduction

The reaction between lime-containing slag and molten metal plays an important role in desulfurization and dephosphorization of molten iron. It is highly desirable that lime could rapidly melt with other flux components to promote the reaction between slag and metal.

A great number of researches have contributed to clarify the mechanisms involved in dissolution of lime into slag and develop the new methods to promote dissolution of lime into slag. Schlitt *et al.*[1] conducted a kinetic study on lime dissolution into CaO-FeO-SiO_2 slag by lowering specimens of CaO into the molten slag for a prescribed time, and then withdrawing them to the upper section of tube to cool. They found that the dissolution rate of lime markedly increased with increasing the FeO content in slag. The mechanism of CaO dissolution into slag was also investigated by observing the lime-containing flux heated on Pt-filament directly through a microscope.[2] It is indicated that the layer of $2CaO \cdot SiO_2$ is formed on the surface of CaO particles, and dissolution of CaO proceeded by migration of the molten slag through cracks on the layer of $2CaO \cdot SiO_2$. In the case of higher Fe_2O_3 content, the layers of $2CaO \cdot SiO_2$ and $3CaO \cdot SiO_2$ compounds formed around the CaO crystal were not continuous but looked more like particles, which promoted dissolution of CaO.[3] The rate of dissolution of solid lime into liquid slag was determined from the decrease in diameter of a lime cylinder rotated in CaO-SiO_2-Al_2O_3 or FeO-CaO-SiO_2 slag.[4] The diffusion of calcium through a slag boundary phase was revealed to be the rate-determining step. By use of a rotating-disc apparatus, influence of lime properties on rate of dissolution in CaO-SiO_2-FeO slag was investigated.[5] The more porous lime was found to show the higher reactivity in the experiments. In addition, influence of various fluxing agents, such as BOF slag and dust, BF slag, on lime dissolution was also studied.[6]

In recent years, there is an increasing concern about environment. Fluorspar(CaF_2) is a commonly used additive to promote melting of lime-containing flux. Owing to fluorine containing species released into the atmosphere and dissolved into the soil from the disposed slag, utilization of fluorspar is increasingly limited. On the other hand, in order to reduce the amount of steelmaking slag, higher reactivity of lime is also strongly demanded. Therefore, the alternative additives and methods are required for facilitating the melting of lime-containing flux.

Lee et al.[7] developed a new flux of burnt lime(CaO) coated with di-calcium ferrite($2CaO \cdot FeO$). It was claimed that this new kind of flux had a high resistance to hydration and a capacity for fast and complete dissolution into the steelmaking slag of BOF and EAF. Hamano *et al* studied dissolution rate[8] of solid lime into the molten slag used for hot-metal dephosphorization, and the reaction mechanism[9] between solid lime and the slag. They concluded that the effect of the additives to Fe_tO-CaO-SiO_2 melt on increasing the dissolution rate of CaO was CaF_2>$CaCl_2$>B_2O_3>Al_2O_3. Amini *et al*[10] indicated that addition of CaF_2, MnO_x, FeO_x, and TiO_2 into

Al_2O_3-CaO-SiO_2 slag increased the dissolution rate of lime into slag, while SiO_2 had an opposite effect.

In contrast to most of the previous studies on dissolution rate of block lime into the molten slag, the present work concentrates on promotion of the melting of CaO-containing flux particles. By use of high temperature optical microscope(HTOM), the melting processes of flux particles are *in situ* observed. The flux melting is also confirmed from observation using a scanning electron microscope (SEM) and analysis with an energy dispersive spectrometer(EDS). The flux melting temperature is determined by a differential scanning calorimeter (DSC). Furthermore, a novel method is proposed to promote the melting of CaO-containing flux, by taking advantage of heat generated by thermit reaction between Fe_2O_3 and Al.

2. Experimental Apparatus and Procedures

The materials used for the experiment were calcium oxide powders (10 μm in average diameter and purity of 99.9%), aluminium oxide powders (50 μm in average diameter and purity of 99.9%), silicon oxide powder(0.8 μm in average diameter and purity of 99.9%), α-iron oxide powders (15 μm in average diameter and purity of 99.5%), and aluminum powder (75－150μm in diameter and purity higher than 99.5%). After mixing, pellets were formed by use of a cold isostatic press(CIP) under a pressure of 150 MPa for one hour, having the diameter of 3 mm and the length of 2 mm.

The components of pellets are shown in Table 1. Run B had the common constitution of slag employed in iron and steel making process, which had a relatively low melting point of about 1573 K from the CaO-Al_2O_3-SiO_2 ternary phase diagram.[11] In Run A, Fe_2O_3 and Al powders were added at the stoichiometric mole ratio of 1:2 according to thermit reaction between Fe_2O_3 and Al. After the thermit reaction, the components of Run A would be almost the same as those in Run B except for iron produced. On the other hand, Run D had the components that are possible to be used as a dephosphorization flux in pretreatment of hot metal and had a low melting point of about 1473 K.[12] In Run C, Al powders were added instead of Al_2O_3 powders in Run D. After thermit reaction between Fe_2O_3 and Al, the constitution of Run C would be almost the same as that in Run D. In Run E, a minimum amount of Al powders was added for compensating the heat absorbed during the flux melting and its temperature rising to the melting point. The calculation method of the addition amount of Al powders will be described in the later part of this paper.

Figure 1 is a schematic diagram of high temperature optical microscope. It has components of a hot stage and an optical microscope equipped with a digital video camera, monitor and computer. The *in-situ* observation of the flux melting process was performed by placing an examining pellet in a platinum crucible of 6.0 mm i.d. and 2.0 mm in height. Then the crucible was set in a sapphire sample holder equipped with B-type thermocouple, and the whole assembly was located in the hot zone of the platinum-image furnace.

Table 1. Pellet components in the experiments.

	CaO (%)	Al_2O_3 (%)	SiO_2 (%)	Fe_2O_3 (%)	Al (%)
Run A	29.6	12.1	32.9	18.8	6.6
Run B	34.0	27.7	38.3	0	0
Run C	18.1	0	0	77.2	4.7
Run D	20.2	8.6	0	71.2	0
Run E	19.5	6.9	0	72.6	1.0

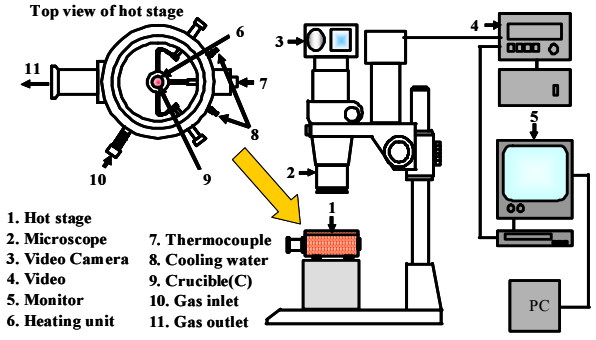

Fig. 1. Schematic diagram of high temperature optical microscope.

Before heating, the chamber was evacuated with a diffusion pump and backfilled with ultrapure Ar gas, in which oxygen and water vapor were minimized by passing through heated Mg chips and a gas-cleaning system. This purified Ar gas at a flow rate of 3.3×10^{-6} m^3/s was also used as the protective gas during the experiment. The sample was observed from top surface through a top quartz window. The temperature on the sample surface was calibrated by use of an optical pyrometer. In Runs A and B, pellet masses were 0.0190 g. In Runs C, D and E, pellets of 0.020 g were used.

After observation with HTOM, the cooled pellet was observed using SEM. The microscopic compositions at various positions on the pellet surface were determined by EDS. The melting temperatures of different kinds of flux were further determined by use of differential scanning calorimeter (DSC).

3. Experimental Results and Discussion

3.1. Melting of CaO-Al_2O_3-SiO_2 Flux Assisted by Thermit Reaction

By use of HTOM, the change in temperature with time is shown in **Fig. 2**. The specimen was heated to 1073 K at the rate of 50 K/min, and then to 1623 K at the rate of 10 K/min. During the heating, it was held for 10 min at the temperatures of 1273, 1373, 1473 and 1573 K.

Figure 3 presents the morphologies of all kinds of materials before formation of pellets. Calcium oxide powders were relatively uniform in diameter. The diameters of aluminium oxide powders were varied, ranging from 20 μm to 80 μm. An aluminum oxide particle was usually in a cluster formed by many fine aluminum oxide particles. Silicon oxide powders were very fine in size with the average diameter of only 0.8 μm. α-iron oxide powders had greatly varied diameters and irregular shapes. Aluminum powders had dense surface with the diameters ranging from 75 μm to 150μm.

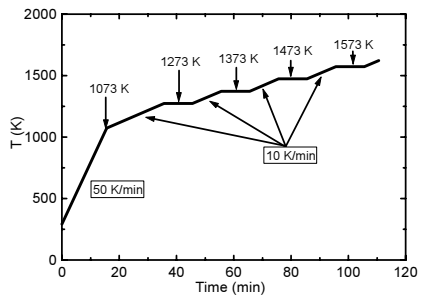

Fig. 2. Change in experimental temperature with time by use of high temperature optical microscope.

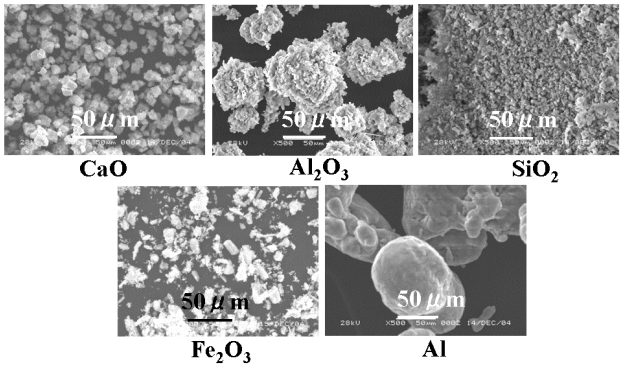

Fig. 3. Morphology and size of each kind of powders to be mixed to form pellets.

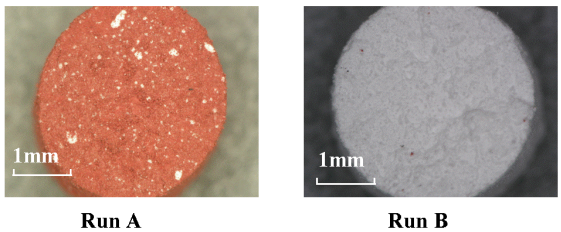

Fig. 4. Optical micrographs of pellet for Run A and B before experiment.

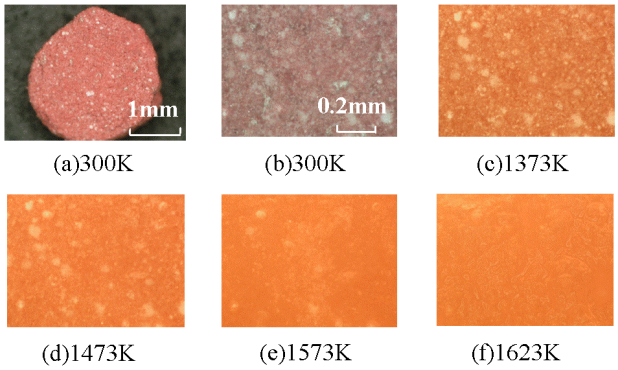

Fig. 5. Change in pellet morphology with temperature (Run A).

The optical microscope images of the whole pellet before the experiment are presented in **Fig. 4**. The pellet had a diameter of 3.5 mm and a height of 1.0 mm. The pellet of Run A had a red color of Fe_2O_3 powders dotted with white color of the other added particles. The pellet of Run B had a gray white color. Both pellets of Runs A and B had a mass of 0.0190 g.

The results of *in situ* observation of melting process of lime-containing flux assisted by thermit reaction for Run A are shown in **Fig . 5**. The frame size is 0.73 mm by 0.97 mm. The morphological change of the pellet was not detected before 1373 K. After rising to 1473 K, the white parts on the pellet surface decreased in their areas. And it was observed that the surface of pellet had begun to move. After rising to 1573 K, the flow on the pellet surface was clearly observed, and the specimen was fully melting.

The thermit reaction between Fe_2O_3 and Al usually involves a highly exothermic reaction along with vigorous combustion.[13-15] However, in the present experiment, the ignition and combustion phenomenon was not observed. This is because the components of CaO, Al_2O_3 and SiO_2 acted as the inactive materials, the reaction heat was deprived and the ignition and combustion were obstructed.

After *in situ* observation, the cooled specimen was further observed with SEM and analyzed with EDS. **Figure 6** shows the results. Before experiment as shown in diagram(a), the individual particle made a distinct appearance. After 10 min holding at 1373 K, a few of the particles were partly melting as shown in diagram(b). The EDS analysis results show that at points of A, B and C, the particles almost remained their original compositions. After 10 min holding at 1473 K, diagram(c) clearly shows that the pellet was fully melting and the individual particle disappeared. The EDS results also show that at points of D and E, all kinds of compositions in the pellet were obviously detected. The melting of pellet was confirmed. These results are in good agreement with those *in situ* observed by use of HTOM, indicating the lime-containing flux was fully melting at the temperature of 1473 K with assistant from thermit reaction.

For comparison, experiment of Run B was conducted. Run B had nearly the same components as those of Run A after thermit reaction. The SEM images and EDS analysis results after experiment are given in **Figure 7**. Before experiment, the particles appeared individually. After 10 min holding at 1473, there was no change in the particle morphology and no sign of melting. After 10 min holding at 1573 K, a few of particles seemed to be partly melting. EDS results shows most of the particles remained their original compositions on the pellet surface. At point C, CaO combined with Al_2O_3. In comparison to Run A, it is clear that the melting of lime-containing flux is greatly promoted with assistant from thermit reaction.

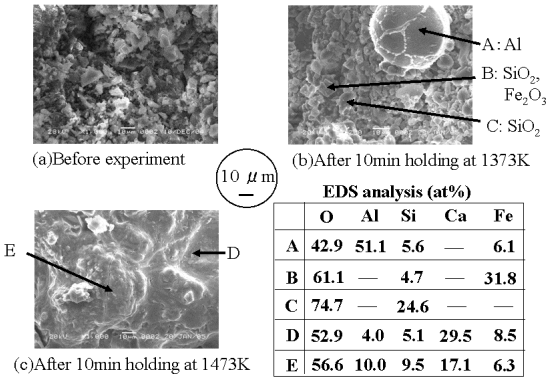

EDS analysis (at%)

	O	Al	Si	Ca	Fe
A	42.9	51.1	5.6	—	6.1
B	61.1	—	4.7	—	31.8
C	74.7	—	24.6	—	—
D	52.9	4.0	5.1	29.5	8.5
E	56.6	10.0	9.5	17.1	6.3

Fig. 6. SEM image and EDS analysis of pellet after experiment(Run A).

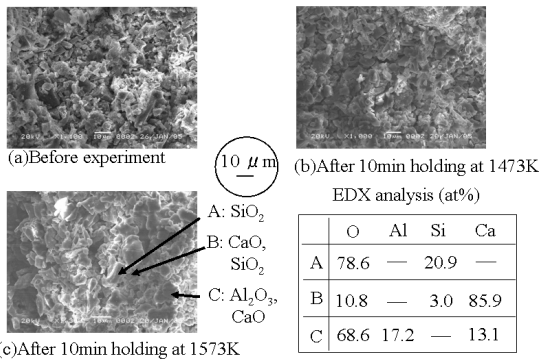

EDX analysis (at%)

	O	Al	Si	Ca
A	78.6	—	20.9	—
B	10.8	—	3.0	85.9
C	68.6	17.2	—	13.1

Fig. 7. SEM image and EDS analysis of pellet after experiment(Run B).

In order to obtain the melting temperature more exactly for Runs A and B, a differential scanning calorimeter(DSC) was used to measure the start melting temperature. The pellet mass was 0.0190 g, which was the same as that in observation with HTOM. A platinum crucible of 6.0 mm i.d. and 2.0 mm in height was used. An inert atmosphere was maintained by use of Ar gas at the flow rate of 8.3×10^{-7} Nm^3/s. The heating rate was 0.167 K/s.

Figure 8 presents the DSC results for Runs A and B. For Run B, initiating from 1587 K, a great endothermic peak appeared. After that, no endothermic peak was detected and the specimen was fully meting after DSC measurement. Therefore, it is clear that the endothermic peak was caused by the flux melting and its start temperature was 1587 K, which was close to the melt point(1573 K) of the ternary $CaO\text{-}Al_2O_3\text{-}SiO_2$ phase of the present components.

For Run A, at 933 K, there was an endothermic peak, which corresponded to melting endotherm of Al. Initiating from 1413 K, a big exothermic peak appeared, which matched the great heat generation of thermit reaction between Fe_2O_3 and Al. After DSC measurement, the specimen was fully melting, but no endothermic peak was further detected. Therefore, it is reasonable to deduce that the flux melting proceeded simultaneously with thermit reaction. The great heat generation of thermit reaction had assisted the melting of lime-containing flux. Since the heat generated during thermit reaction was much greater than that absorbed during flux melting, the exothermic peak was due to the surplus heat of thermit reaction after compensating the heat absorption of flux melting. The start melting temperature in Run A was decreased to 1413 K, which was much lower than that in Run B. Again, it is confirmed that the melting of lime-containing flux was greatly promoted with assistance from thermit reaction.

3.2. Melting of $CaO\text{-}Al_2O_3\text{-}Fe_2O_3$ Flux Assisted by Thermit Reaction

The melting of dephosphorization flux assisted by thermit reaction was further studied. The components of pellets are shown in Table 1. Run D had the constitution of common dephosphorizaiton flux. In Run C, Al powders were added instead of Al_2O_3 powders. The optical microscope images of the whole pellet before the experiment are presented in **Fig. 9**. The pellet had a diameter of 3.5 mm, a height of 1.0 mm and a mass of 0.020 g. Both pellets had red color of the Fe_2O_3 powders dotted with white color of the other added particles.

For Run C, change in pellet morphology with temperature *in situ* observed by HTOM is given in **Fig. 10**. After 873 K, the color of the pellet surface changed from red to grey. This is maybe due to the partial decomposition of Fe_2O_3. Before 1443 K, no obvious change in morphology was detected. When the temperature was raised to 1523 K, the flow caused by the melting of pellet was observed on its surface. The pellet was fully melting.

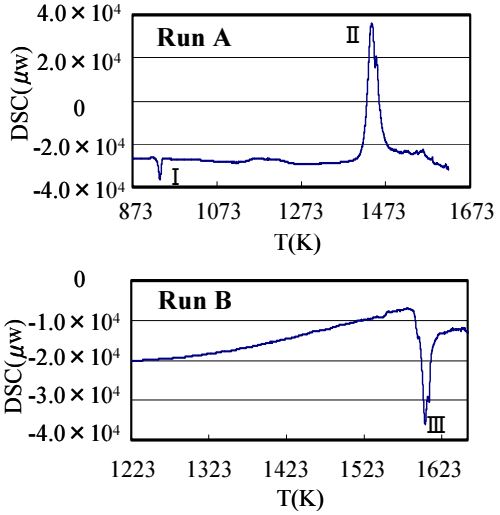

Fig. 8. DSC results of Run A and B.

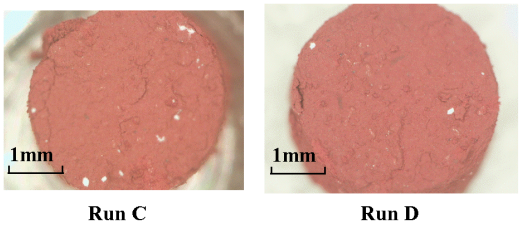

Fig. 9. Optical micrographs of pellet for Run C and D before experiment.

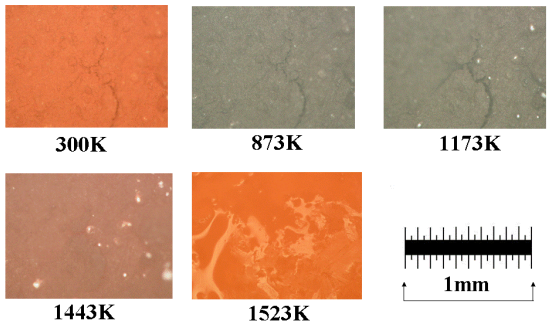

Fig. 10. Change in pellet morphology with temperature(Run C).

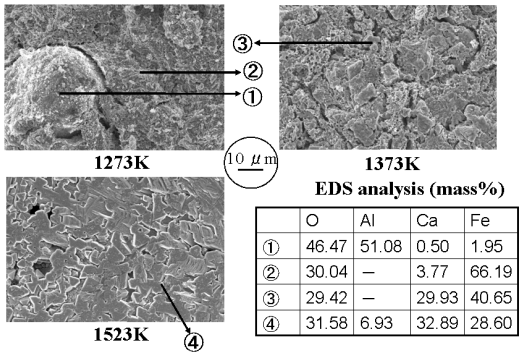

EDS analysis (mass%)

	O	Al	Ca	Fe
①	46.47	51.08	0.50	1.95
②	30.04	–	3.77	66.19
③	29.42	–	29.93	40.65
④	31.58	6.93	32.89	28.60

Fig. 11. SEM image and EDS analysis of pellet after experiment(Run C).

Figure 11 shows the SEM images and EDS analysis results for cooled pellets of Run C after they were heated to different temperatures. After heated to 1273 K, the pellet was not melting, which could be justified from the appearance of pellet. From EDS analysis results, just a slight combination between CaO and Fe_2O_3 could be recognized. After heated to 1373 K, the pellet was partly melting, which could be identified from the gaps formed by melting contraction. EDS results also show that CaO and Fe_2O_3 were well amalgamated. After heated to 1523 K, the pellet was fully melting. CaO and Fe_2O_3, as well as Al_2O_3 were completely amalgamated.

For comparison, pellets of Run D, in which Al powders were not added, were also heated for SEM observation and EDS analysis. The results are shown in **Fig. 12**. After heated to 1273 K, the morphology of pellet did not show it melting. EDS analysis indicates that a slight amalgamation between CaO and Fe_2O_3 took place. After heated to 1373 K, the pellet did not look like melting. But CaO and Fe_2O_3 were somewhat amalgamated from the EDS results. After heated to 1523 K, the pellet showed partly melting. But some particles appeared individually without melting, which could be justified from the appearance of pellet. The EDS results indicate that at some parts on the pellet surface, CaO, Fe_2O_3 and Al_2O_3 are amalgamated.

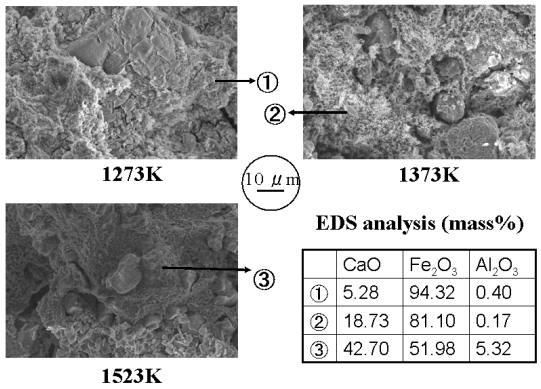

EDS analysis (mass%)

	CaO	Fe_2O_3	Al_2O_3
①	5.28	94.32	0.40
②	18.73	81.10	0.17
③	42.70	51.98	5.32

Fig. 12. SEM image and EDS analysis of pellet after experiment(Run D).

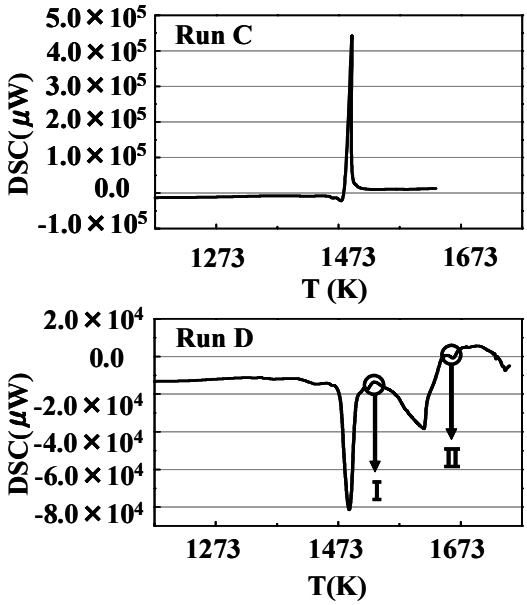

Fig. 13. DSC results of Run C and D.

The DSC measurement was also conducted for Runs C and D as shown in **Fig. 13**. The measurement conditions were the same as those for Runs A and B except for heating rate of 0.50 K/s. For Run D, the first endothermic peak began at the temperature of 1470 K. From the binary CaO-Fe_2O_3 phase diagram,[12] since the eutectic temperature is about 1473 K, the first peak should correspond to the amalgamation between CaO and Fe_2O_3. The second endothermic peak initiated from 1553, which should match the amalgamation of all the three components in the pellets. The point Ⅰ of 1538 K is the temperature just after the first peak and before the second peak, while point Ⅱ of 1663 K is the temperature after the second peak. After heated to temperatures of Ⅰ and Ⅱ, the cooled samples were further observed with SEM and analyzed with EDS. The results are given in **Fig. 14**. After heated to temperature Ⅰ, the SEM image clearly shows some of white particles did not melt, and their compositions were mainly Al_2O_3. It can be seen that at this temperature, CaO and Fe_2O_3 were well amalgamated. After heated to temperture Ⅱ, at every point on the pellet surface, CaO and Fe_2O_3, as well as Al_2O_3 were fully melting. Therefore, it is confirmed that the first peak in Fig. 13(RunD) was caused by the amalgamation between CaO and Fe_2O_3, while the second peak corresponded to the entire melting of pellet. The fully melting temperature was obtained to be 1663 K

The DSC analysis result for Run C is also shown in Fig. 13. Since there was only an exothermic heat peak and the specimen was fully melting after the measurement, it is clear that flux melting proceeded simultaneously with thermit reaction. The exothermic heat peak was attributed to the surplus heat of thermit reaction after compensating the endothermic heat of flux melting. The start temperature of the exothermic reaction was 1478 K, which was lower than the initiating temperature of 1553 K for the entire melting in Run D. The fully melting temperature of 1503 K is much lower than that of 1663 K without assistance from thermit reaction. This means that the melting of dephosphorization flux is also promoted with assistance from thermit reaction.

3.3. Estimation of Heat Generation by Thermit Reaction

In order to obtain the minimum addition amount of Al powders for melting the flux in Run C, heat generated by thermit reaction is estimated. It is assumed that the heat generated by thermit reaction does not escape from the reaction system, being used only for flux melting and its rising in temperature, and the products do not disintegrate.

The thermit reaction between Fe_2O_3 and Al can be described as

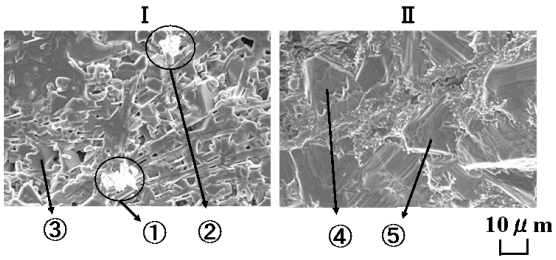

	CaO	Fe_2O_3	Al_2O_3
①	—	1.68	98.32
②	2.66	0.75	96.59
③	42.70	57.30	—

EDS analysis (mass%)

	CaO	Fe_2O_3	Al_2O_3
④	30.59	54.24	15.17
⑤	25.56	38.96	35.48

Fig. 14. SEM image and EDS analysis of pellet after DSC measurement(Run D).

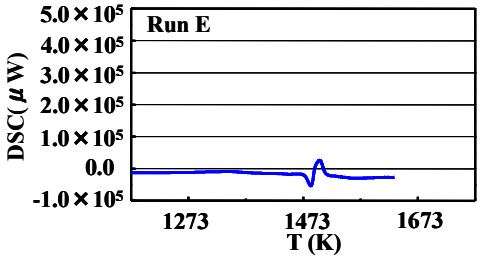

Fig. 15. DSC results of Run E.

$$2Al + Fe_2O_3 \rightarrow 2Fe + Al_2O_3 \quad \text{……..(1)}$$

If x mol Al powders are added, one can obtain

$$x\,Al + \frac{x}{2}Fe_2O_3 \rightarrow \; x\,Fe + \frac{x}{2}Al_2O_3 \quad \text{……..(2)}$$

From the DSC analysis, it is known that the peak temperature for thermit reaction is 1493 K for Run C and the melting point of Al is 933 K,[16] the heat generated by thermit reaction can be estimated as

$$\Delta H^{\circ}_{(2)} = \frac{x}{2} \times \Delta H^{\circ}_{298(2)} + \int_{298}^{933} \Delta C_{p(2)} dT - x \times \Delta H_{m(Al)} + \int_{933}^{1493} \Delta C_{p(2)'} dT \quad \text{……..(3)}$$

where

$$\Delta H^{\circ}_{298(2)} = \Delta H^{\circ}_{298,Al_2O_3} - \Delta H^{\circ}_{298,Fe_2O_3} \quad \text{……..(4)}$$

$$\Delta C_{p(2)} = x \cdot C_{p,Fe} + \frac{x}{2} C_{p,Al_2O_3} - x \cdot C_{p,Al(s)} - \frac{x}{2} \cdot C_{p,Fe_2O_3} \quad \text{……..(5)}$$

$$\Delta C_{p(2)'} = x \cdot C_{p,Fe} + \frac{x}{2} C_{p,Al_2O_3} - x \cdot C_{p,Al(l)} - \frac{x}{2} \cdot C_{p,Fe_2O_3} \quad \text{……..(6)}$$

$\Delta H_{m(Al)} = 8.4(\text{kJ})$,[16] $\Delta H^{\circ}_{298,Al_2O_3}$ =-1677.4(kJ/mol), $\Delta H^{\circ}_{298,Fe_2O_3}$ =-821.3(kJ/mol), $C_{p,Fe(s)}$, $C_{p,Al_2O_3(s)}$, $C_{p,Fe_2O_3(s)}$ and $C_{p,Al(l)}$ are the molar specific heat of each component.[17] As a result, $\Delta H^{\circ}_{(2)}$ =-451.815x kJ/mol.

On the other hand, the components in Run D have a molar raito of $CaO:Fe_2O_3:Al_2O_3$=4:5:1. If x mole of Al powders is added into pellets, and the products have the same component as that in Run D, the molar ratio of $CaO:Fe_2O_3:Al_2O_3$:Al in the pellets should be 4:(5+x/2):(1-x/2):x. After thermit reaction, the molar ratio of $CaO:Fe_2O_3:Al_2O_3$:Fe in the product becomes 4:5:1:x.

From the DSC results, Run D has a melting point of about 1623 K, which is taken as the second peak temperature in Fig. 13. After thermit reaction, as for the product having a molar ratio of $CaO:Fe_2O_3:Al_2O_3$:Fe = 4:5:1:x, the necessary heat for pellet melting and its temperature rising from 1493 K to 1623 K is

$$\Delta H^{\circ}_{(P)} = \int_{1493}^{1623} (4 \times C_{p,CaO} + 5 \times C_{p,Fe_2O_3} + C_{p,Al_2O_3} + x \cdot C_{p,Fe}) dT + \Delta H_{m(CaO-Fe_2O_3-Al_2O_3)} \quad \text{……..(7)}$$

Where $\Delta H_{m(CaO\text{-}Fe_2O_3\text{-}Al_2O_3)}$=61.294 kJ, which is obtained by DSC analysis for the present specimen, $C_{p,CaO}$, C_{p,Fe_2O_3}, C_{p,Al_2O_3} and $C_{p,Fe}$ are the molar specific heat of each component. As a result, $\Delta H^{\circ}_{(p)} = 201.562 + 6.074x$ (kJ).

If the heat generated by thermit reaction($\Delta H^{\circ}_{(2)}$) is equal to the necessary heat for pellet melting and its temperature rising from 1493 K to 1623 K, the minimum amount of Al powders is x=0.451 (mol). And the mass percent ratio at this component is $CaO:Fe_2O_3:Al_2O_3$:Al=19.5:72.6:6.9:1.0. This means that only if 1.0% of Al powder is added, the flux will be fully melting after thermit reaction.

The components of Run E have a mass percent ratio of $CaO:Fe_2O_3:Al_2O_3$:Al=19.5:72.6:6.9:1.0. The DSC measurement for Run E was conducted as shown in **Fig. 15**. After the measurement, the specimen was fully melting. Moreover, both of the endothermic and exothermic peaks were very small, indicating that the heat generated by thermit reaction just compensated the heat absorbed by the flux melting and its temperature rising. This is in good agreement with the predication made above.

4. Conclusions

A new method for promoting the melting of lime-containing flux is proposed with assistance from thermit

reaction between Fe_2O_3 and Al. Two kinds of fluxes are used. One has the component of CaO-Al_2O_3-SiO_2, having a common constitution of slag employed in iron and steel making process. The other has the component of CaO-Al_2O_3-Fe_2O_3, which is possibly used for dephosphorization in the pretreatment of hot metal. The flux melting process is *in situ* observed by use of High Temperature Optical Microscope(HTOM). The cooled samples are further observed by SEM, and analyzed by EDS. Furthermore, the heat change in the process is determined by differential scanning calorimeter (DSC). Following conclusions can be drawn from the present studies:

1) For the first kind of flux of the component of CaO-Al_2O_3-SiO_2, its melting initiates from the temperature of 1587 K. With assistance from thermit reaction between Fe_2O_3 and Al, the start melting temperature is decreased to 1413 K. The results of the flux melting *in situ* observed by use of HTOM are in good agreement with those measured with DSC. The SEM-EDS results indicate that after holding 10 min at 1473 K, the flux is fully melting and all of the components in the flux are amalgamated assisted by thermit reaction.
2) For the second kind of flux of the component of CaO-Al_2O_3-Fe_2O_3, it is revealed that the melting process take place in two stages. At the first stage, CaO is combined with Fe_2O_3; at the second stages, they are further amalgamated with Al_2O_3. The fully melting temperature is decreased from 1663 K to 1503 K with assistance from thermit reaction between Fe_2O_3 and Al.
3) An estimation of heat generation during thermit reaction is carried out. The minimum amount of Al powders necessary for assistance of the flux melting is obtained. The result of testifying experiment is in a good agreement with the prediction result.

Acknowledgement

This study was supported in part by JFE 21st Century Foundation, Grants-in-Aid for Scientific Research in 2006-2007.

Reference

1. W. J. Schlitt and G. W. Healy: *Am. Ceram. Soc. Bull.*, **50**(1971), 954.
2. H. Kimura, T. Yanagase, F. Noguchi and Y. Ueda: *J. Jpn. Inst. Met.*, **38**(1974), 226.
3. F. Noguchi, Y. Ueda and T. Yanagase: *J. Jpn. Inst. Met.*, **41**(1977), 883.
4. M. Matsushima, S. Yadoomaru, K. Mori and Y. Kawai: *Trans. ISIJ*, **17**(1977), 442.
5. C. A. Natalie and J. W. Evans: *Ironmaking Steelmaking*, **6**(1979), 101.
6. M. H. Chiang, G. I. Yang, H. Y. Chang, T. F. Lee and R. Dasgupta: *Am. Ceram. Soc. Bull.*, **67**(1988), 1222.
7. M. Lee and P. Barr: *Steel Research*, **73**(2002), 123.
8. T. Hamano, M. Horibe and K. Ito: *ISIJ Int.*, **44**(2004), 263.
9. T. Hamano, S. Fukagai and F. Tsukihashi: *ISIJ Int.*, **46**(2006), 490.
10. S. H. Amini, M. P. Brungs, S. Jahanshahi and O. Ostrovski: Metall. *Mater. Trans. B*, **37B**(2006), 773.
11. The Iron and Steel Institute of Japan: Tekkoubinran(Handbook of Iron and Steel)(Ⅰ), Maruzen, 1981, 47.
12. E. M. Levin, C. R. Robbins and H. F. Mcmurdie: Phase Diagrams for Ceramists, The American Ceramic Society, Columbus, USA, 1964, 49.
13. O. Menekse, J. V. Wood and D. S. Riley: *Materials Science and Technology*, **22**(2006), 199.
14. R. Seshadri: *Materials and Manufacturing Process*, **17**(2002), 501.
15. D. G. Kim, J. Kaneko and M. Sugamata: *Journal of The Japan Institute of Metals*, **57**(1993), 679.

16. The Japan Institute of Metals: Databook of Metal, Maruzen, Tokyo, Japan, 1974, 10.
17. S. Ban-ya: Ferrous Process Metallurgy, The Japan Institute of Metals, Sendai, Japan, 2000, 233.